

# Anisotropic Scattering Rates in the $t - t' - U$ Hubbard Model

Joachim Altmann<sup>1</sup>, Wolfram Brenig<sup>1</sup>, and Arno P. Kampf<sup>2</sup>

<sup>1</sup> *Institut für Theoretische Physik, Universität zu Köln,  
Zùlpicher Str. 77, 50937 Köln, Germany*

<sup>2</sup> *Theoretische Physik III, Elektronische Korrelationen und Magnetismus,  
Universität Augsburg, D-86135 Augsburg, Germany*

We have investigated the evolution of the electronic properties of the  $t$ - $t'$ - $U$  Hubbard model with hole doping and temperature. Due to the shape of the Fermi surface, scattering from short wavelength spin fluctuations leads to strongly anisotropic quasi-particle scattering rates at low temperatures near half-filling. As a consequence, significant variations with momenta near the Fermi surface emerge for the spectral functions and the corresponding ARPES signals. This behavior is quite in contrast to the intermediate doping regime and we discuss the possible relevance of our results for the interpretation of photoemission spectra in cuprate superconductors at different hole doping levels.

PACS numbers: 74.72.-h, 75.50.Ee, 79.60.-i

A key issue in the efforts to understand the microscopic physics of high- $T_c$  superconductors is the evolution of the electronic properties with doping. In recent years theoretical work has continuously benefited from angular resolved photoemission spectroscopy (ARPES) data for the electronic spectrum and the Fermi surface in the normal state as well as for the anisotropic energy gap in the superconducting state [1]. In particular, remarkable recent ARPES results for the underdoped cuprates have shown an anisotropic normal-state pseudogap which forms below  $\sim 150\text{K}$  for the weakly underdoped materials increasing up to  $\sim 300\text{K}$  for the heavily underdoped compounds with a  $T_c$  close to zero [2–5]. Contrary to optimally doped and overdoped samples the quasi-particle peak in the underdoped spectra is found to be very weak near the  $(\pi, 0)$  point of the Brillouin zone (BZ) and no Fermi surface crossing is observed on the BZ boundary along the  $(\pi, 0)$  to  $(\pi, \pi)$  direction. Furthermore the spin susceptibility [6],  $c$ -axis optical [7] as well as in-plane infrared conductivity [8], NMR relaxation rates [9], and inelastic neutron scattering data [10] indicate a pseudogap in the low-energy excitation spectrum of underdoped compounds. Different scenarios like pair formation well above  $T_c$  [11,12], spin-charge separation [13,14] or precursor effects near the antiferromagnetic (AF) instability [15,16] have been proposed as possible origins of these pseudogap phenomena.

In this paper, we explore the combined effects of strong spin fluctuation scattering and Fermi surface topology using the 2D Hubbard model on a square lattice with a  $t - t'$  dispersion of the one-particle kinetic energy

$$\epsilon_{\mathbf{k}} = -2t(\cos k_x + \cos k_y) - 4t' \cos k_x \cos k_y \quad (1)$$

with nearest-neighbor ( $t$ ) and next-nearest neighbor ( $t'$ ) hopping amplitudes. Near half-filling we demonstrate that strong quasi-particle scattering rates develop with decreasing temperature near the so called “hot spots” on the Fermi surface (FS), i.e. FS points which are con-

nected by the AF wave vectors  $\mathbf{Q} = (\pm\pi, \pm\pi)$ . As a consequence of the emerging highly anisotropic scattering rates the quasi-particle peaks in the spectral functions near the  $(\pi, 0)$  points of the BZ are suppressed in comparison to the momenta near  $\mathbf{k}_F$  along the BZ diagonal leading to highly anisotropic ARPES signals.

Our method of choice to evaluate the renormalized one-particle excitations is the self-consistent and conserving [17] fluctuation-exchange (FLEX) approximation [18]. In this approach the self-energy is given in terms of the spin- and density-fluctuation  $T$ -matrices  $T_{sf}(\mathbf{r}, \tau)$  and  $T_{\rho\rho}(\mathbf{r}, \tau)$  by

$$\Sigma(\mathbf{r}, \tau) = U^2 G(\mathbf{r}, \tau) [\chi_0(\mathbf{r}, \tau) + T_{\rho\rho}(\mathbf{r}, \tau) + T_{sf}(\mathbf{r}, \tau)] \quad (2)$$

where  $\chi_0(\mathbf{r}, \tau) = -G(\mathbf{r}, \tau)G(-\mathbf{r}, -\tau)$  is the particle-hole bubble and  $\mathbf{r}$  and  $\tau$  denote real space coordinates and imaginary time, respectively.  $U$  is the on-site Coulomb repulsion. The Fourier transformed  $T_{sf}(\mathbf{q}, i\omega_m)$  and  $T_{\rho\rho}(\mathbf{q}, i\omega_m)$  are defined by

$$T_{\rho\rho}(\mathbf{q}, i\omega_m) = -\frac{1}{2} \frac{U\chi_0^2(\mathbf{q}, i\omega_m)}{1 + U\chi_0(\mathbf{q}, i\omega_m)} \quad (3)$$

$$T_{sf}(\mathbf{q}, i\omega_m) = \frac{3}{2} \frac{U\chi_0^2(\mathbf{q}, i\omega_m)}{1 - U\chi_0(\mathbf{q}, i\omega_m)} \quad (4)$$

where  $\omega_m = 2m\pi T$  are the bosonic Matsubara frequencies at temperature  $T$ . In combination with Dyson’s equation  $G^{-1} = G_0^{-1} - \Sigma$ , Eqs. (1), (2), and (3) form a self-consistent set of equations which we solve numerically by iteration. One of the keys to the numerical solution is the *locality* of (2) in space and time as well as the *locality* of (3) and (4) in momentum and frequency space. This allows for a completely algebraic treatment of the FLEX iterations by repeated application of intermediate Fast-Fourier-transforms [19]. The proper *stability* of the self-consistent cycle is achieved by solving the FLEX equations on a contour in the complex frequency plane

which is shifted off the real axis by a finite amount  $i\gamma$  with  $0 < \gamma < \pi T/2$  [21]. Analytic continuation to the real frequency axis does not encounter the usual problems of purely imaginary frequency methods [19].

We have solved the FLEX equations on lattices with up to  $128 \times 128$  sites using an equally spaced frequency mesh of 4096 points within an energy window of  $[-30t, 30t]$ . The lower bound on the temperature accessible in our present calculations is  $T \sim 0.02t$ . This bound is set by the smallest width in frequency space of the AF paramagnon-peak in  $\text{Im } T_{sf}(\mathbf{q}, \omega + i\gamma)$  which can be resolved for the chosen frequency mesh as well as the smallest momentum space width which can be treated without introducing finite size effects. Throughout the paper we will adopt an interaction strength  $U = 4t$  and  $t' = -0.3t$  – a parameter set for which the Hubbard model exhibits long range AF order in the ground state at half-filling [20].

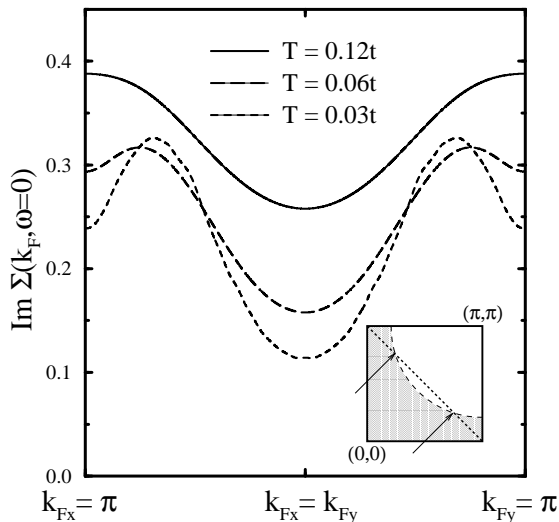


FIG. 1.  $\text{Im } \Sigma(\mathbf{k}_F, \omega = 0)$  along the Fermi line for various temperatures  $T$  with  $U = 4t$ ,  $t' = -0.3t$  and hole doping  $\delta = 2.5\%$ . The inset shows schematically the Fermi line (dashed line) and the “hot spots” (arrows) in one quarter of the BZ.

We start with the discussion of our results by considering the FS anisotropy of the one-particle scattering rate for small hole concentrations. Its momentum dependence is governed by two effects: First, the available recoil phase-space which is linked to the momentum-space width of the AF paramagnon peak in  $\text{Im } T_{sf}(\mathbf{q}, \omega)$  and second the density of intermediate states. While the former quantity exhibits a variation with temperature and doping which discriminates only weakly between the  $t$ - and the  $t$ - $t'$  model in the low doping limit, the latter quantity depends crucially on the  $t$ - $t'$  band structure. This is a major source of difference between the one-particle renormalizations in the  $t$ - and  $t$ - $t'$  Hubbard models. In particular, we observe a non-trivial temperature and momentum dependence of the one-particle

self-energy. This is shown in Fig. 1 which depicts the imaginary part of  $\Sigma(\mathbf{k}, \omega = 0)$  along the FS line, i.e. at  $\mathbf{k} = \mathbf{k}_F$ . For  $T \gtrsim 0.08t$  the AF peak in  $\text{Im } T_{sf}(\mathbf{q}, \omega)$  is a relatively broad structure, i.e. its HWHM in momentum and frequency space is  $\sim \pi/6$  and  $\sim 0.2t$ , respectively. Therefore, in essence,  $\Sigma(\mathbf{k}_F, \omega = 0)$  is modulated only by the density of states along the FS which is largest at the borders of the BZ and smallest at the point  $\mathbf{k}_{F\gamma}$  on the BZ diagonal, i.e. where  $k_{Fx} = k_{Fy}$ . For decreasing temperatures the peak in  $\text{Im } T_{sf}(\mathbf{q}, \omega)$  at the AF wave vector  $\mathbf{q} = \mathbf{Q}$  sharpens until we loose its accurate resolution at about  $T \approx 0.02t$ . This redistribution of weight shifts the maximum in  $\text{Im } \Sigma(\mathbf{k}_F, \omega = 0)$  into the so-called “hot spots” on the FS which can be connected by the AF wave vector. In addition to this shift the low-temperature anisotropy of the self-energy is enhanced by roughly a factor of two.

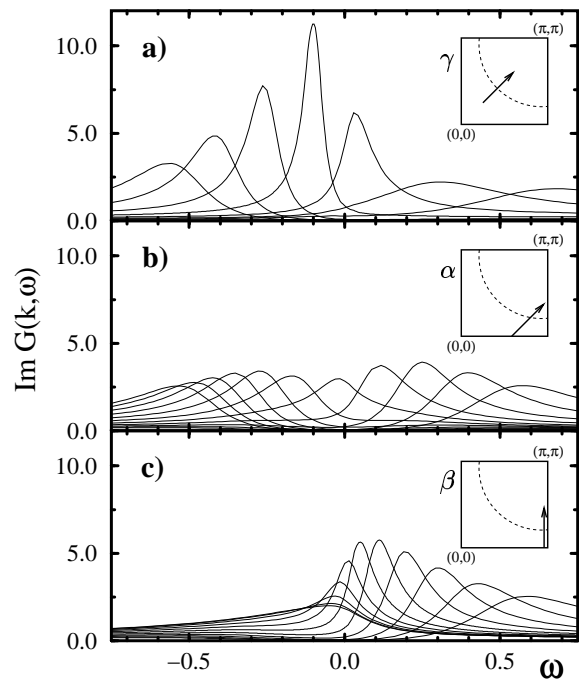


FIG. 2.  $\text{Im } G(\mathbf{k}, \omega)$  along three different paths in the BZ – schematically shown in the insets – for  $T = 0.03t$ ,  $U = 4t$ ,  $t' = -0.3t$  and  $\delta = 2.5\%$  on a  $64 \times 64$  lattice. The path  $\gamma$  in a) is chosen along the BZ diagonal from  $\mathbf{k}_\gamma = (11, 11)\frac{\pi}{32}$  to  $(17, 17)\frac{\pi}{32}$ . In b) the path  $\alpha$  is parallel to the path in a) but runs from  $\mathbf{k}_\alpha = (21, 0)\frac{\pi}{32}$  to  $(32, 11)\frac{\pi}{32}$  crossing the (hot spot) maximum of  $\text{Im } \Sigma(\mathbf{k}_F, \omega = 0)$  at  $\mathbf{k}_{F\alpha} \approx (26, 5)\frac{\pi}{32}$ . The path  $\beta$  in c) is along the BZ boundary from  $\mathbf{k}_\beta = (32, 0)\frac{\pi}{32}$  to  $\mathbf{k}_{\beta} = (32, 11)\frac{\pi}{32}$ .

In Fig. 2 we show the consequence of the anisotropic scattering rates for the single-particle spectral function at  $T = 0.03t$ . Choosing a path in momentum space as shown in Fig. 2a) which crosses the FS at  $\mathbf{k}_{F\gamma}$ , i.e. the wave vector of the minimal scattering rate, a well defined, sharp quasi-particle peak is observed. In contrast, the quasi-particle feature is strongly suppressed in Fig. 2b) where the FS is traversed by passing through a hot

spot. In comparison to Fig. 2a) the amplitude of the quasi-particle peak near  $\mathbf{k}_F$  is reduced by almost a factor of three and, moreover, it is *minimal on the FS*. Finally, choosing a path which cuts the FS on the BZ boundary as in Fig. 2c), the quasi-particle structure is asymmetrically distributed as a function of momentum being more pronounced in the inverse photoemission sector. Only weak dispersion of the quasi-particle peak below the Fermi energy along this cut signals a “flat-band” region close to the momentum  $(\pi, 0)$ . We note that ARPES spectra can be obtained from Fig. 2a)–c) by multiplying  $\text{Im } G(\mathbf{k}, \omega)$  with the Fermi function. Only near the momentum  $\mathbf{k}_{F\gamma}$  these spectra are found to display well defined quasi-particles which disperse through the Fermi energy, while the quasi-particle weight in the vicinity of the hot spots and the BZ boundary is substantially reduced.

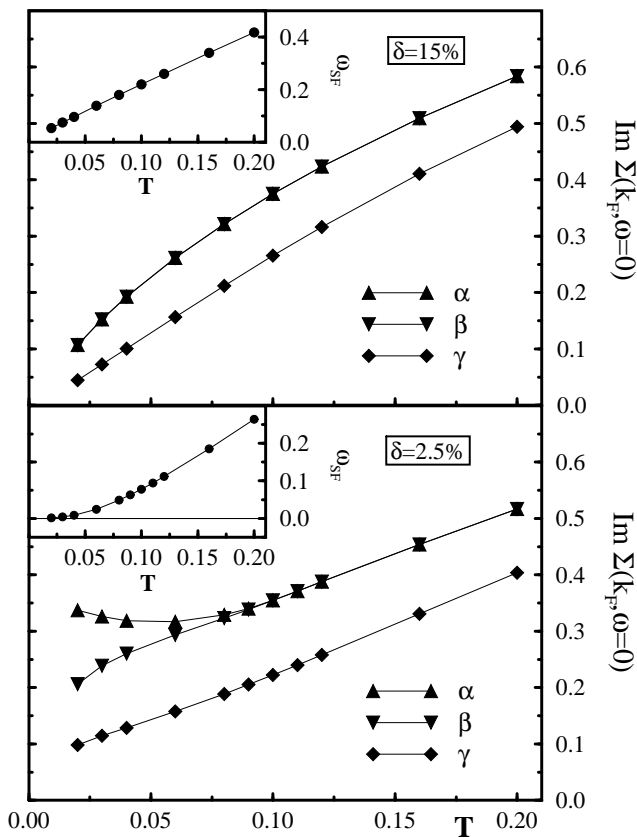


FIG. 3.  $\text{Im } \Sigma(\mathbf{k}_F, \omega=0)$  for three points on the Fermi line (at maximal scattering rate, i.e.  $\mathbf{k}_{F\alpha}$ , as well as  $\mathbf{k}_{F\beta}$ , and  $\mathbf{k}_{F\gamma}$  as defined in the caption of Fig. 2) and hole dopings of 15% and 2.5% in the temperature range  $T = [0.02t; 0.2t]$ . The insets display the temperature dependence of the spin fluctuation energy scale  $\omega_{sf}$ .

Fig. 3 summarizes the temperature dependence of the imaginary part of the on-shell ( $\omega = 0$ ) self-energy at the FS for two doping concentrations  $\delta = 15\%$  and  $2.5\%$  for Fermi momenta on the BZ boundary, the BZ diagonal, and the momentum of the maximal scattering rate, i.e.

$\mathbf{k}_{F\beta}$ ,  $\mathbf{k}_{F\gamma}$ , and  $\mathbf{k}_{F\alpha}$ , respectively. While for  $\delta = 15\%$  the momenta  $\mathbf{k}_{F\alpha}$  and  $\mathbf{k}_{F\beta}$  coincide at all temperatures depicted they *separate* below a critical temperature  $T^*$  for  $\delta = 2.5\%$ . Therefore, the ‘ $\alpha$ -self-energy’ in Fig.3b) contains both, an explicit temperature dependence as well as an implicit one which is linked to the movement with temperature of  $\mathbf{k}_{F\alpha}(T)$  along the FS line.

Two conclusions can be drawn from Fig. 3. First, we observe an intimate relation between the temperature  $T^*(\delta)$  and the spin fluctuation frequency  $\omega_{sf}(T)$  which we define by the frequency of the maximum in  $\text{Im } T_{sf}(\mathbf{q}, \omega)$  at  $\mathbf{q} = \mathbf{Q}$ . The insets show the temperature dependence of  $\omega_{sf}$  for both doping concentrations. Hot spots start to form once the temperature drops *below* the spin-fluctuation frequency scale, i.e. when  $T^*(\delta) \sim \omega_{sf}(T)$ . We find that this scenario is valid at all doping levels which we have investigated and moreover that  $T^*(\delta)$  increases with decreasing doping concentrations. It is clearly tempting to relate  $T^*(\delta)$  with the pseudogap formation temperature observed in ARPES [2–5] and optical conductivity experiments [8].

As a second consequence Fig. 3 suggests the existence of a very small energy scale which is manifest in the self-energy at low doping. At  $\delta = 15\%$   $\text{Im } \Sigma(\mathbf{k}_f, \omega = 0)$  clearly extrapolates to zero for vanishing temperatures at all FS momenta. This is consistent with Fermi-liquid theory (FLQ). However, at  $\delta = 2.5\%$  a similar behavior can not be anticipated. This pertains to all momenta irrespective of the additional upturn of the scattering rate at  $\mathbf{k}_{F\alpha}$  below  $T^*(\delta)$  which is partially due to the temperature dependent shift of  $\mathbf{k}_{F\alpha}(T)$ . In order to recover low-temperature FLQ behavior we are forced to assume that  $\text{Im } \Sigma(\mathbf{k}_{F\alpha}(T), \omega = 0, T)$  will approach zero below a second characteristic temperature  $T^{FLQ}(\delta)$  below  $T^*(\delta)$ . Since  $\omega_{sf}(T)$  is the only characteristic low-energy scale available it is natural to assume that  $T^{FLQ}(\delta) \sim \omega_{sf}(T^{FLQ}(\delta))$ . As is obvious from the inset of Fig. 3b) this temperature is expected to be very small for  $\delta = 2.5\%$  and remains inaccessible within the numerical accuracy of our present computational scheme.

Finally we show the quasi-particle dispersion for  $\delta = 15\%$  and  $2.5\%$  in Fig. 4. The quasi-particle energies have been determined from the zeroes of the real part of the inverse Green function, i.e. from  $E(\mathbf{k}) = \epsilon(\mathbf{k}) - \text{Re } \Sigma(\mathbf{k}, E(\mathbf{k}))$ . Far off the Fermi energy this figure seems to suggest a nearly rigid-band picture. However, close to the FS the situation is less trivial, in particular close to the wave vector  $\mathbf{k} = (\pi, 0)$ , where quasi-particle energies get strongly renormalized. With decreasing doping concentrations we find the flat band region around this wave vector to be ‘pinned’ to the Fermi energy and – surprisingly – deformed towards a stronger dispersion. While for  $\delta = 15\%$  the quasi-particle energy  $E(\pi, 0) \simeq -1.09t$  is very close to the bare energy of  $\epsilon(\pi, 0) = -1.20t$ , the pinning gives rise to a substantial renormalization at  $\delta = 2.5\%$  where we find  $E(\pi, 0) \simeq -0.73t$ . Qualitatively similar pinning, however quantitatively less pronounced, can be observed along the BZ diagonal.

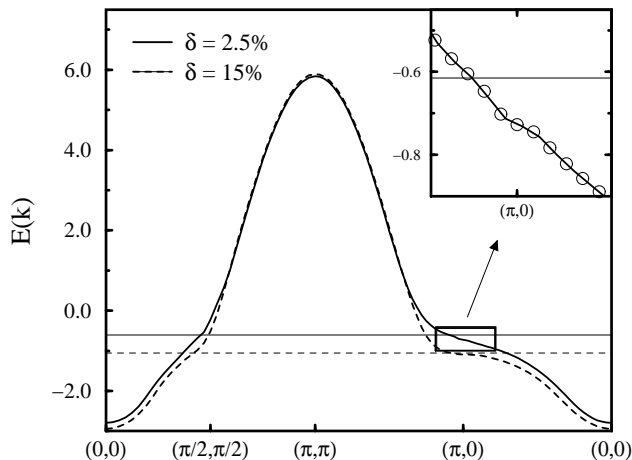


FIG. 4. Quasi-particle dispersion relation for two different hole doping concentrations along the closed path in the BZ  $(0,0) \rightarrow (\pi,\pi) \rightarrow (\pi,0) \rightarrow (0,0)$ . The horizontal lines indicate the chemical potentials for both doping levels. The inset shows a magnification of the vicinity of the  $(\pi,0)$  point.

Focusing on the low-energy sector in the vicinity of the Fermi surface the inset in Fig. 4 details yet another remarkable, though weak effect. While a continuous band dispersion is evident from this inset, with a well defined Fermi surface crossing on the BZ boundary, the quasi-particle energy develops a step like feature around  $(\pi,0)$  for  $\delta = 2.5\%$ . This is a precursor of the energy gap opening at half-filling and induces a pseudogap structure in the density of states. We have verified this feature to be robust against finite size scaling on up to  $128 \times 128$  lattices. Clearly the magnitude of the pseudogap is too small to account for the recent corresponding findings of ARPES [2–5]. A tempting remedy for this deficiency is to decrease the ratio of  $|t'/t|$  and thereby enhance the effects of nesting. Indeed, within our FLEX scheme, we found that reducing  $t'$  leads to a pronounced increase of the pseudogap structure and moreover to the appearance of a split-off precursor band similar to that observed in ARPES [22]. This is also consistent with QMC data obtained on the pure  $t$ -model [23]. However, we believe that this route to pseudogap behavior is inconsistent, both with the Fermi surface topology of the cuprate materials as well as with the strong anisotropy of the quasi-particle scattering rate, which both require the inclusion of a finite hopping amplitude  $t'$ . Therefore a proper understanding of the combined effects of anisotropy and pseudogap formation requires further investigations.

In conclusion we have studied the anisotropic electronic properties of the two-dimensional  $U - t - t'$  Hubbard model which result from the unique combination of the shape of the Fermi surface and strong scattering from spin fluctuations. With decreasing hole doping and lowering of the temperature hot spots develop on the Fermi surface with significantly enhanced scattering rates offering a physical explanation for the observed strong anisotropies of the ARPES signals in the under-

doped cuprates. For realistic values of the ratio  $t'/t$  clear Fermi surface crossings are still maintained in our FLEX calculation and therefore a pronounced pseudogap formation is not obtained. An extension to bilayer type Hubbard models is a possible path for further study since the bilayer splitting into a bonding and an antibonding band provides another important low energy scale which may be of particular relevance near the  $(\pi,0)$  point of the BZ.

This research was performed within the program of the Sonderforschungsbereich 341 supported by the Deutsche Forschungsgemeinschaft (DFG).

- 
- [1] For a review see Z.-X. Shen and D. Dessau, Phys. Rep. **253**, 1 (1995).
  - [2] D.S. Marshall et al., Phys. Rev. Lett. **76**, 4841 (1996).
  - [3] A.G. Loeser et al., Science **273**, 325 (1996).
  - [4] H. Ding et al., Nature **382**, 51 (1996).
  - [5] H. Ding et al., Phys. Rev. **B52**, R9678 (1996).
  - [6] M. Oda et al., Physica C **183**, 234 (1991).
  - [7] C.C. Homes et al., Phys. Rev. Lett. **71**, 1645 (1993).
  - [8] D.N. Basov et al., Phys. Rev. Lett. **77**, 4090 (1996); A.V. Puchkov et al., Phys. Rev. Lett. **77**, 3212 (1996).
  - [9] M. Takigawa et al., Phys. Rev. **B43**, 247 (1991).
  - [10] J. Rossat-Mignod et al., Physica **B169**, 58 (1991).
  - [11] S. Doniach und M. Inui, Phys. Rev. **B41**, 6668 (1990); Y. Uemura et al., Phys. Rev. Lett. **66**, 2665 (1991); M. Randeria et al., Phys. Rev. Lett. **69**, 2001 (1992).
  - [12] V.J. Emery and S.A. Kivelson, Nature **374**, 434 (1995); J. Ranninger and J.-M. Robin, Phys. Rev. **B53**, 11961 (1996); J. Mały et al., preprint cond-mat/9609083 and references therein.
  - [13] H. Fukuyama, Prog. Theo. Phys. Suppl. **108**, 287 (1992).
  - [14] X.G. Wen and P. Lee, Phys. Rev. Lett. **76**, 503 (1996).
  - [15] Z.-X. Shen and J. R. Schrieffer Phys. Rev. Lett. **78**, 1771 (1997).
  - [16] A.V. Chubukov et al., preprint cond-mat/9606208; D. Pines, preprint cond-mat/9702187.
  - [17] G. Baym, Phys. Rev. **127**, 1391 (1962).
  - [18] N.E. Bickers and D.J. Scalapino, Annals of Physics **193**, 206 (1989).
  - [19] J.W. Serene and D.W. Hess, in *Recent Progress in Many-Body Theories*, Vol. 3, T.L. Ainsworth et al., Eds., Plenum Press, New York (1992), and references therein.
  - [20] D. Duffy and A. Moreo, Phys. Rev. **B52**, 15607 (1995).
  - [21] Schmalian et al., Comp. Phys. Comm. **93**, 141 (1996).
  - [22] J. Altmann, W. Brenig, and A.P. Kampf, unpublished.
  - [23] R. Preuss et al., preprint cond-mat/9701097.